International Journal of Research in Engineering and Science (IJRES)
ISSN (Online): 2320-9364, ISSN (Print): 2320-9356
www.ijres.org Volume 4 Issue 10 ǁ October. 2016 ǁ PP.08-19

Nonlinear Versatile Tools for Heart Rate Variability Prediction andDiagnosis

Mazhar B. Tayel[1], Eslam I Alsaba[2]
[1,2]*Electrical Engineering Department, Faculty Of Engineering., Alexandria University, Alexandria, Egypt*

Abstract : Heart rate variability (HRV) refers to variations in heart complex wave beat- to-beat intervals. The HRV is a reliable reflection of many physiological, psychological, and environmental factors modulating the normal rhythm of the heart. In fact, the HRV seriously provides a powerful means of observing the interplay between the sympathetic and parasympathetic nervous systems. However, the HRV has a periodicity that is important for monitoring and following up the cases. The structure generating heart complex wave signal is not simply linear, but it also involves nonlinear contributions. These contributions are totally correlated. .
The HRV is stochastic and chaotic (stochaotic) signal. It has utmost importance in heart diseases diagnosis, and it needs a sensitive tool to analyze its variability. The present work introduces and discusses some methods to be used for analysis and prediction of HRV. Also, explain a novel reliable methods to analyze the linear and nonlinear behaviour of the heart complex wave variability, to assess the use of the HRV as a versatile tool for heart disease diagnosis. The Mazhar-Eslam Variability Frequency MVF "Ω_M"is the most versatile tool for HRV prediction and diagnosis that discussed in this thesis. The MVF "Ω_M" diversity of initially closely trajectories in state-space is connected with folding of them. The presence of a positive part MVF for all initial conditions in a restricted dynamical system, is the vastly used definition of deterministic chaos. Thus, to distinguish between periodic signals chaotic and dynamics, the MVF Ω_M are predominantly used. The trajectories of chaotic signals in state-space pursue typical patterns. Nearly diverge trajectories diverge and converge exponentially, proportional to each other. A negative MVF means that the orbit entices to a settled point or stable periodic orbit. Negative MVFs are distinguishing of non-fogyish systems. Like systems display asymptotic stability. For more stability, the MVF is more negative. When MVF tends to infinity, it is mean the excessive stable periodicity. Thus, it is clear that the MVF is the most suitable and sensitive tool for predicting the HRV. Morever, it discusses the Poincare limitation, cause of standard deviation SD1, SD2 and how to overcome this limitation by using complex correlation measure (CCM). The CCM is most sensitive to changes in temporal structure of the Poincaré plot as compared toSD1 and SD2**.**

Keywords : Linear methods, Nonlinear methods, Heart Rate Variability (HRV), Poincaré Plot, Mazhar-Eslam Variability Frequency (MVF).

I. INTRODUCTION

Heart rate variability (HRV) is define as the inter-beat variability between successive heart beats in a determined time interval. This variability is mediated directly by polarization and depolarization process of sinus node. Which at the same time is regulated by interaction of the sympathetic and parasympathetic branches of autonomic nervous system (ANS). An increase in the parasympathetic activity means decreasing in heart rate (HR) by release of acetylcholine, however, an increase of HR is a direct consequence of an increase in the sympathetic activity which in this case is mediate through norepinephrine release on heartbeat regularity mechanism [1, 2, 3]. So, it can be established that the dynamical balance between sympathetic and parasympathetic activity has strong effect on HR causing vibration around its average value which called HRV phenomenon. Thus, HRV is a noninvasive method to evaluate the sympathetic and parasympathetic function of ANS and cardiovascular system [1]. Figure 1 explain the effect of sympathetic and parasympathetic system on HR beside the outcome of their interaction.

II. GENERATION OF HRV SIGNAL

The heart rate variability (HRV) signals are result of quantifying the distance between successive heartbeats for certain period of time. These periods are estimated by analyzing the electrocardiography (ECG) signals. Practically, the R peak method is the most accurate to identify the all QRS complexes of ECG signal cause of its proficiency in distinguish from other component of complex. Thus, there are several methods for detecting R peaks, some of them based on Hilbert transform [4], signal filtering (pan-tompkins algorithm) [2,3,5], pattern recognition [6], and wavelet transform [7]. Although the accuracy of these methods, there is no standard methodology of R peak detection.

With all R peaks detected, the next step is calculating the difference time between two successive R peaks in order to generate a time series of R-R intervals. After calculation these defrences for the entire signal, the obtained result is a discrete time series called as RR tachogram or HRV signal [3]. It is important to note that this series of variability lacks uniformity in the distance between the points due to temporary differences between successive heartbeats. Figure 2 represents the R-R time series generating from ECG signal [2, 3].

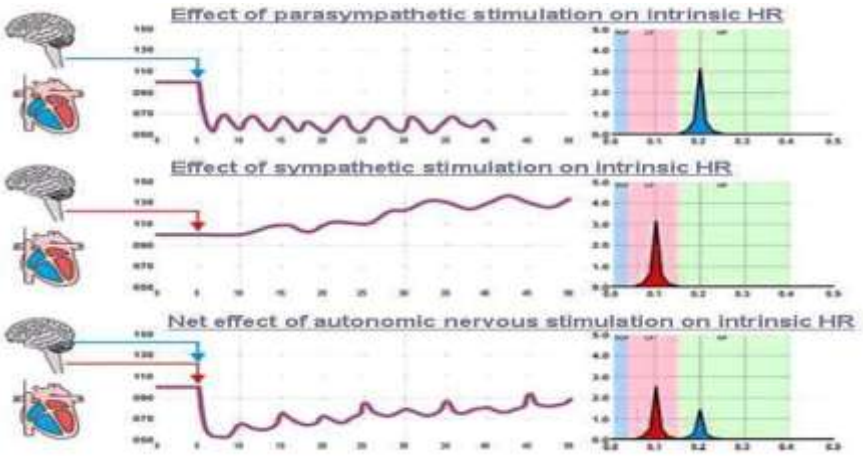

Figure 1. The effect of sympathetic and parasympathetic system on HR

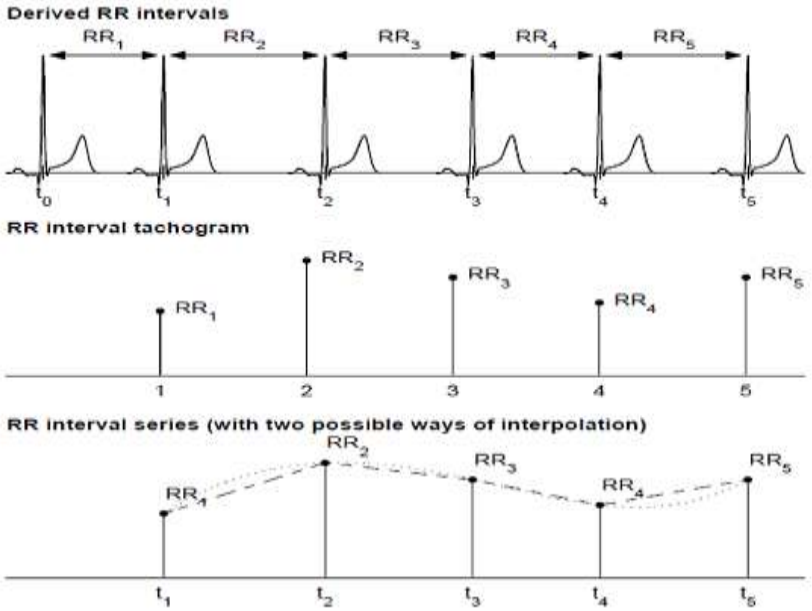

Figure 2. R-R time series generating from ECG signal

III. ASSESSMENT OF THE HRV SIGNAL

The HRV analysis is performed through a combination of linear and nonlinear method. Linear methods have been categorized as methods in time domain and methods in frequency domain, while nonlinear methods correspond to a set of techniques to study the nonlinear dynamics of HRV series.

The analysis in time domain is the simplest way to extract features of HRV signals by quantifying some indexes based on the statistics of signal data. They are the average value of all R-R intervals (AVRR), standard deviation of all R-R intervals (SDNN), root mean square differences of successive R-R intervals (rMSSD), and percentage of differences between N-N intervals that by more than 50ms (pNN-50). It is important to state that previous studies have shown that these time parameters are highly correlated with high frequency variation in HR[2].

HRV signals exhibit an oscillatory behavior in that components of high and low frequency as a result of cardiovascular modulations performed by sympathetic and parasympathetic nervous systems are mixed. Thus, methods of analysis in the frequency domain are used in order to quantify this type of information from estimate the power spectrum as a function of signal frequencies. The calculation of the power spectrum of the

power spectrum density (PSD) of HRV signal can performed using parametric and nonparametric methods. Parametric methods usually estimate power spectrum through autoregressive models applied to the signal. But, nonparametric methods using algorithm based on Fourier transform. However, these methods require that the input signal will be evenly sampled. It means that all samples will be equally spaced in time. Then, in order to fulfill this requirement, it is necessary to perform a process of resampling on the R-R series before the spectral estimations. For HRV series, it is recommended to construct a cubic spline interpolation over the data using a resampling frequency [3]. To avoid resampling process over the HRV signals and obtained PSD estimated directly from unevenly data, the algorithm proposed by Lomb [8] and Scargle [9] can be used. Once the PSD is estimated, it is possible to quantify reliable information in the frequency domain integrating the spectrum in frequency bands. Three frequency bands, related to some physiological phenomena, have been considered as a standard values in the frequency analysis of HRV [2, 10, 11, 12]. The values of these frequency bands correspond to (VLF) band in the range (0.01-0.05 Hz), the second band is low frequency (LF) band in the range (0.06 -0.15 Hz) and the third band is a high frequency (HF) band in the range (0.16-0.50 Hz) as illustrated in figure 3.

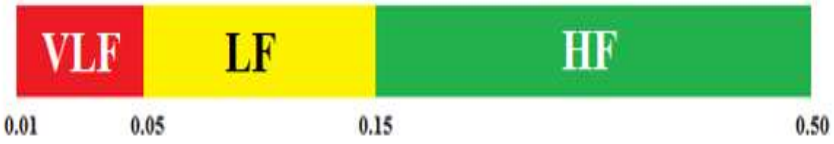

Figure 3. HRV spectrum bands

In addition to the methods of analysis in the time and frequency domain, there are nonlinear methods which have been demonstrated to extremely useful due to the nonstationary characteristics of HRV signals. Most of these methods have their foundation in chaos theory and nonlinear dynamics which allows to analyze HRV signals in more complete way. The most commonly used nonlinear methods for HRV analysis are slope of regression line, Fractal dimension, Detrended Fluctuation Analysis (DFA), Approximate entropy (AppEn), sample entropy (SampEn), Correlation dimension (CD), Hurst exponent (H), Recurrence plots, Lyapunov exponent, PoincaréPlots, and Mazhar-Eslam Variability Frequency [3]. In the next, discussion of the most important and sensitive tools for heart disease diagnosis which are PoincaréPlots, and Mazhar-Eslam Variability Frequency.

IV. POICARÉ PLOT

The Poincaréplot analysis is a geometrical and non-linear method to assess the dynamics of heart rate variability (HRV). The Poincaréplot is a representation of a time series into a phase space, where the values of each pair of successive elements of the time series define a point in the plot. The theoretical background that supports the use of a phase space is the Takens theorem [13]. According to Takens, it is possible to reconstruct the attractor of a dynamical system by mapping a scalar measurement into a phase space using a given time delay and embedding dimension [14]. T

hePoincaréplot in HRV is a scatter plot of the current R-R interval plotted against the preceding R-R interval. It was constructed at a period of intervals before, for example 5 minutes. This method is described by the following formula: Two adjacent RR intervals represent one point in the plot. The first RR interval (RR i) represents the x-coordinate, the second interval (RR i+1) represents y-coordinate. Figure 4 shows a Poincaréplot of a healthy patient. However, the assessment and standardization of these qualitative classifications are difficult because they are highly subjective. A quantitative analysis of the HRV attractor displayed by the Poincaréplot can be made by adjusting it to an ellipse. For the performance analysis, the SD1 (Standard Deviation1), SD2 (Standard Deviation 2) and area of ellipse are used as evaluation parameters [14]. The definitions are given in the next:

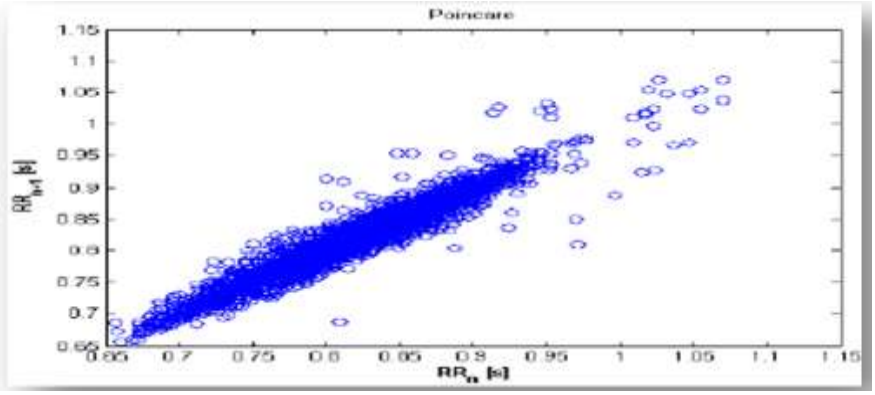

Figure 4. Poincaréplot of a healthy patient

i. *SD1: Standard Deviation 1*

Is the standard deviation (SD) of the instantaneous (short term) beat-to-beat R-R interval variability (minor axis of the ellipse or SD1). SD1 can be calculated as:

$SD1 = \sqrt{var(x_1)}$

ii. ***SD2:*** *Standard Deviation 2*

Is the standard deviation (SD) of the long term R-R interval variability (major axis of the ellipse or SD2). SD2 can be calculated as:

$SD2 = \sqrt{var(x_2)}$

wherevar(*x*) is the variance of variable *x*, and

$x_1 = \frac{\overrightarrow{RR_i} - \overrightarrow{RR_{i+1}}}{\sqrt{2}}$

$x_2 = \frac{\overrightarrow{RR_i} + \overrightarrow{RR_{i+1}}}{\sqrt{2}}$

$\overrightarrow{RR_i}$ and $\overrightarrow{RR_{i+1}}$ are vectors defined as:

$\overrightarrow{RR_i} = (RR_1, RR_2, \dots, RR_{N-1})$

$\overrightarrow{RR_{i+1}} = (RR_2, RR_3, \dots, RR_N)$

Thus, it means, the x_1 and x_2 correspond to the rotation of $\overrightarrow{RR_i}$ and $\overrightarrow{RR_{i+1}}$ by angle $\frac{\pi}{4}$

$$\begin{bmatrix} x_1 \\ x_2 \end{bmatrix} = \begin{bmatrix} \cos\frac{\pi}{4} & -\sin\frac{\pi}{4} \\ \sin\frac{\pi}{4} & \cos\frac{\pi}{4} \end{bmatrix} \cdot \begin{bmatrix} RR_i \\ RR_{i+1} \end{bmatrix}$$

iii. ***Area of Ellipse (S)***

Is the amount of area covered by the ellipse. It can be calculated by doing the product of π, SD1 and SD2 as:

$S = \pi \, . SD1 \, . SD2$

The next example of calculations for Poincarédepend on the ECG signals of healthy and patient subjects taken from fantasia database as shown in Table 1 and Table 2. The SD1 and SD2 are in ms.

Table 1. SD1 and SD2 of Patient Person

Case	SD1	SD2	S
1	32.9287	120.0742	12415.2062
2	21.8979	61.7105	4243.17732
3	25.2745	52.9018	4198.3885
4	21.3007	33.9414	2270.14332
5	15.7004	79.8127	3934.70673
6	23.2662	66.9031	4887.66404

Table 2. SD1 and SD2 for Normal Person

Case	SD1	SD2	S
1	45.4924	117.4879	16782.69254
2	52.8311	133.4969	22145.75455
3	36.8274	126.5634	14635.54300
4	96.0846	268.1668	80907.43709
5	78.8477	159.1354	39399.02527
6	39.0706	138.8992	17040.38776

From Table 1 and Table 2 it is clear that, the Poincaréin normal case represent the statistical value bigger than in diseases case. The Poincaréplot in HRV is widely used to detect and monitoring many important and critical diseases especially in the congestive heart failure (CHF) and cancer cause of its sensitivity.

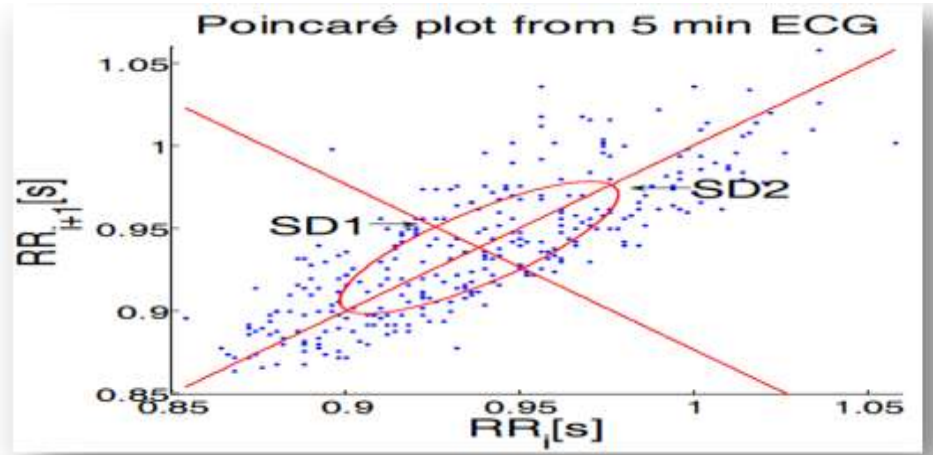

Figure 5. Poincaréplot from a 5 min record of ECG signal from before tilt in a healthy person

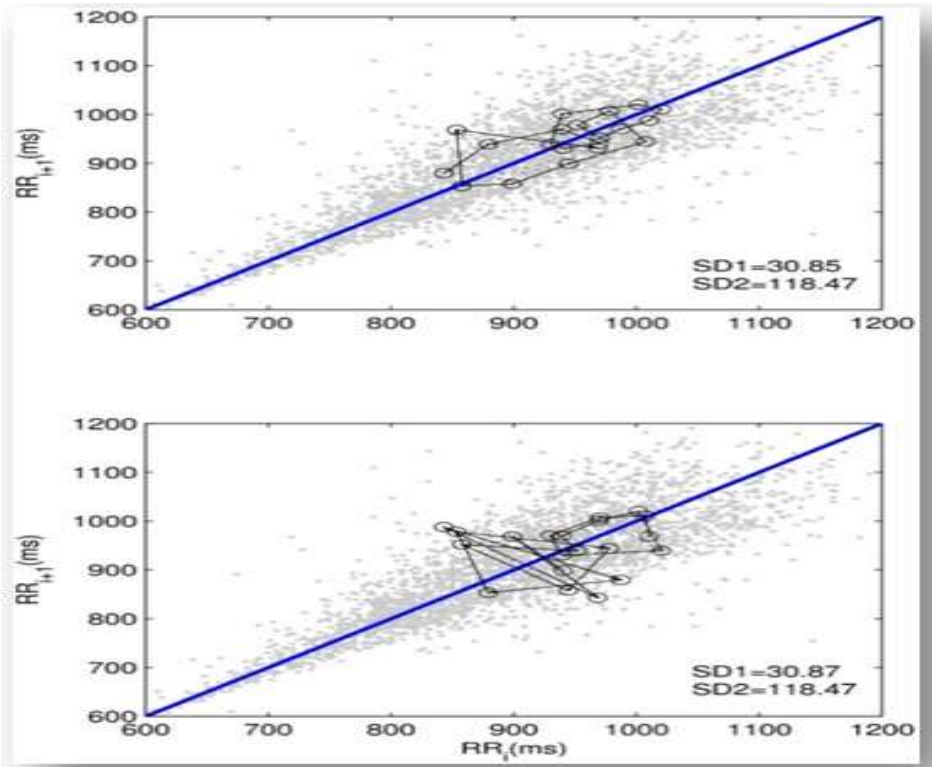

Figure 6. Poincaré plots with similar SD1 and SD2 having different temporal dynamics. Two different RR interval time series of length N (N = 2000) with similar SD1 and SD2 values having different temporal dynamics (first 20 points) are shown in top and bottom panel [15].

The typical shape of a Poincaréplot is an elongated cloud of points around the line-of identity as shown in figure 5.

Although the Poincaréis useful visual pattern for HRV, it has limitations. The primary limitation of the standard descriptors used for quantifying Poincaréplot is the lack of embedding temporal information. The standard deviations, *SD*1 and *SD*2, represent the distribution of signal in two dimensional space and carries only information of width and length. The Poincaréplots of similar *SD*1 and *SD*2 values can have completely different underlying temporal dynamics as shown in figure7 [16]. The complex correlation measure (CCM) is used to overcome this limitation. The CCM is used to quantify the temporal variation of the Poincaré plot. In addition, *CCM* is more sensitive to changes in temporal structure of the signal than *SD*1 and*SD*2.

V. COMPLEX CORRELATION MEASURE

The CCM evaluates point-to-point variation of a signal plotted in a Poincaréplot. Moreover, CCM is a function of multiple lag correlation of the signal [17]. The CCM computed in a windowed manner, which embeds the temporal information of the signal. A moving window of three consecutive points from the Poincaréplot is considered and the area of the triangle formed by these three points is computed. This area measures the temporal variation of the points in the window. If three points are aligned on a line then the area is zero, which represents the linear alignment of the points. Moreover, since the individual measure involves three points of the two dimensional plot, it is comprised of at least four different points of the time series for lag $m = 1$ and at most six points in case of lag $m \geq 3$. Hence, the measure conveys information about four different lag correlation of the signal. Now, suppose the *i-th* window is comprised of points $a(x1, y1)$,$b(x2, y2)$ and $c(x3, y3)$ then the area of the triangle (A) for i[th] window can be computed using the following determinant [17]:

$$A(i) = \frac{1}{2}\begin{vmatrix} x1 & y1 & 1 \\ x2 & y2 & 1 \\ x3 & y3 & 1 \end{vmatrix}$$

where A is defined on the real line $\Re$ and

$$= 0, if points a, b and care on a straight line$$
$$A(i) > 0, counter clock - wise orintation the points a, b, and c$$
$$< 0, clockwise orinatation of the points a, b and c$$

If Poincaréplot is composed of N points then the temporal variation of the plot, termed as CCM, is composed of all overlapping three points' windows and can be calculated as:

$$CCM(m) = \frac{1}{S(N-1)}\sum_{i=1}^{N-2}\|A(i)\|$$

where m represents lag of Poincaréplot. A(i) represents area of the *i-th* triangle. The length of major and minor axes of the ellipse are 2*SD*1, 2*SD*2, where *SD*1, *SD*2 are the dispersion perpendicular to the line of identity (minor axis) and along the line of identity (major axis) respectively.

i. Sensitivity ToChanges In Temporal Structure

Literally, the sensitivity is defined as the rate of change of the value due to the change in temporal structure of the signal. The sensitivity of CCM was analyzed in order to define how it was affected by increasing amount of change in temporal structure [15]. By increasing the number of replacement points the probability of the amount of change in temporal structure of time-series signal should be increased. At each step, number of replaced points is increased by 50. The SD1, SD2 and CCM of a RR interval signal are calculated by increasing number of replacing points at a time. For a selected number of replacing points, it should be shuffled the points for 30 times and calculated all descriptors each time after shuffling. Finally, the replaced values of descriptors were taken as a mean of the calculated values. Now the sensitivity of descriptors ΔSD1j, ΔSD2j and ΔCCMj was calculated using the next:

$$\Delta SD1_j = \frac{SD1_j - SD1_0}{SD1_0} \times 100\%$$
$$\Delta SD2_j = \frac{SD2_j - SD2_0}{SD2_0} \times 100\%$$
$$\Delta CCM_j = \frac{CCM_j - CCM_0}{CCM_0} \times 100\%$$

where $SD1_0$, $SD2_0$ and CCM_0 were the parameters measured for the original data set without replacement and j represents the window number whose data was replaced. Moreover, SD1j, SD2j and CCMj represent the SD1, SD2 and CCM values respectively after replacement of j[th] step.

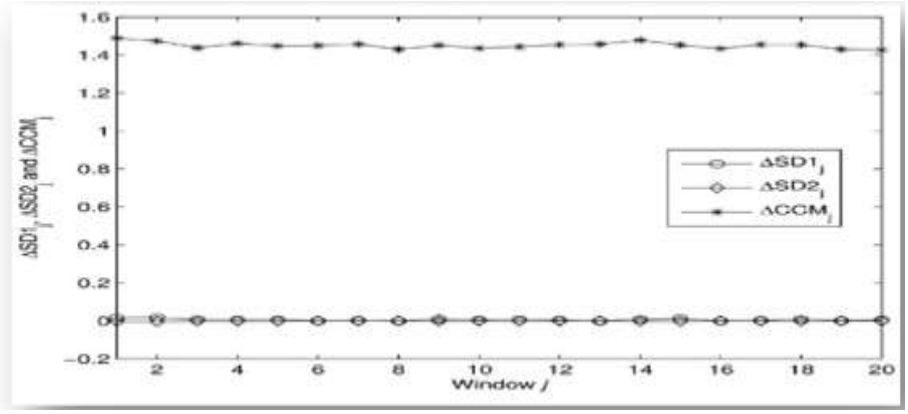

Figure 7. Sensitivity of descriptors with changed temporal structure

Figure 7 shows the sensitivity of all descriptors with change in temporal structure. Δ*SD*1, Δ*SD*2 and Δ*CCM* are calculated using the equations (5.27), (5.28) and (5.29). Value of Δ*CCM* is much higher than Δ*SD*1 and Δ*SD*2, which indicates that *CCM*is much more sensitive than *SD*1 and *SD*2 to the changes in underlying temporal structure of the data.

VI. THE MAZHAR-ESLAM ALGORITHM

The Mazhar-Eslam [1, 18] algorithm uses Discrete Wavelet Transform (DWT) considering the merits of DWT over that of FFT. Although the FFT has been studied extensively, there are still some desired properties that are not provided by FFT. There are some points are lead to choose DWT instead of FFT. The first point is hardness of FFT algorithm pruning. When the number of input points or output points are small comparing to the length of the DWT, a special technique called pruning is often used [19]. However, it is often required that those non-zero input data are grouped together. FFT pruning algorithms does not work well when the few non-zero inputs are randomly located. In other words, sparse signal does not give rise to faster algorithm.

The other disadvantages of FFT are its speed and accuracy. All parts of FFT structure are one unit and they are in an equal importance. Thus, it is hard to decide which part of the FFT structure to omit when error occurring and the speed is crucial. In other words, the FFT is a single speed and single accuracy algorithm, which is not suitable forsensitive dependence (SED) cases.

Moreover, the other reason for not selecting FFT is that there is no built-in noise reduction capacity. Therefore, it is not useful to be used. According to the previous ,the DWT is better than FFT especially in the SED calculations used in HRV, because each small variant in HRV indicates the important data and information. Thus, all variants in HRV should be calculated.

The Mazhar-Eslam algorithm depends to some extend on Rosenstein algorithm's strategies to estimate lag and mean period, and uses the Wolf algorithm for calculating the MVF (Ω_M) except the first two steps, whereas the final steps are taken from Rosenstein's method. Since the MVF (Ω_M) measures the degree of the SED separation between infinitesimally close trajectories in phase space, as discussed before, the MVF (Ω_M) allows determining additional invariants. Consequently, the Mazhar-Eslam algorithm allows to calculate a mean value for the MVF (Ω_M), that is given by

$$\overline{\Omega_M} = \sum_{i=1}^{j} \frac{\Omega_{M\,i}}{j}$$

Note that the Ω_{M_i}s contain the largest Ω_{ML} and variants Ω_Ms that indicate to the helpful and important data. Therefore, the Mazhar-Eslam algorithm is a more SED prediction quantitative measure. Therefore, it is robust quantitative predictor for real time, in addition to its sensitivity for all time whatever the period.

Apply the Mazhar-Eslam algorithm to the HRV of the normal case, it is found that the mean MVF ($\overline{\Omega_M}$) as 0.4986 Hz, which is more accurate than Wolf (0.505 Hz) and Rosenstein (0.7586 Hz).**Figure 8** shows the flowchart for calculating the Mazhar-Eslam MVF algorithm.

First Start to select an initial condition. An embedded point in the attractor was randomly selected, which was a delay vector with d_E elements. A delay vector generates the reference trajectory (nearest neighbor vector). Then another trajectory is selected by searching for the point that minimizes the distance to the particular reference point. After that the divergence between the two vectors is computed. A new neighbour vector was consideredas the evolution time was higher than three sample intervals. The new vector was selected to minimize the length and angular separation with the evolved vector on the reference trajectory. The steps are repeated until the reference trajectory has gone over the entire data sample. The divergence and $\Omega_{Li}s$ are calculated. Consequently,theΩ_M is calculated.

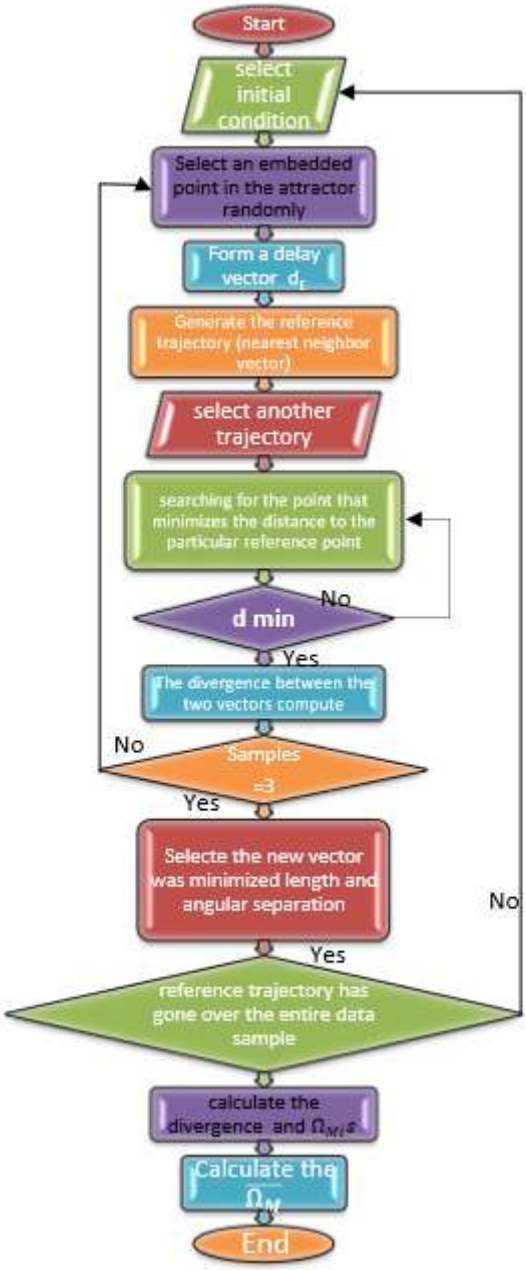

Figure 8. The flowchart of the Mazhar-Eslam algorithm.

VII. Discussions

The introduced MVF "Ω_M" divergence of initially SED nearby trajectories in state-space is coupled with folding of trajectories. To discriminate between stochaotic dynamics, periodic, and aperiodic signals, the MVF "Ω_Ms" are often to be used as a qualitative measure of SED. The trajectories of stochaotic signals in state-space follow typical patterns. Closely spaced trajectories converge and diverge exponentially, relative to each other. Therefore, the existence of a positive MVF ($\Omega_M > 0$) for almost all initial conditions in a bounded dynamical system is to be used for the deterministic stochaotic HRV cases.

Table 3 shows the spectrum bands of the normal HRV and some cases from MIT-BIH database, using the three algorithms: Mazhar-Eslam, Wolf, and Rosenstein, used to compare the SED precision of the three algorithms in determining the MVF.

It is worth to note that the introduced Mazhar-Eslam algorithm spectral analysis of the given HRV reveals three distinct frequency bands in the modulation of humans HRs. The first band is very low frequency (VLF) band in the range (0.01-0.05 Hz), the second band is low frequency (LF) band in the range (0.06 -0.15 Hz) and the third band is a high frequency (HF) band in the range (0.16-0.50 Hz) as illustrated in figure 3. These results coincides with that mentioned in [20].

Table 3. The MVF results of different methods using normal case and MIT-BIH sample cases.

Parameter		MVF		
Serial	**Method** **Case**	**Rosenstein**	**Wolf**	**Mazhar-Eslam**
1	Normal	**0.7586 (HF)**	**0.505 (HF)**	**0.4986 (HF)**
2	101	**0.2500 (HF)**	**0.1700 (HF)**	**0.0830 (LF)**
3	102	**0.1600 (HF)**	**0.1300 (LF)**	**0.0530 (VLF)**
4	104	**0.2100 (HF)**	**0.1300 (LF)**	**0.0700 (LF)**
5	106	**0.2300 (HF)**	**0.1500 (LF)**	**0.0770 (LF)**
6	107	**0.2000 (HF)**	**0.1300 (LF)**	**0.0667 (LF)**
7	109	**0.2200 (HF)**	**0.1400 (LF)**	**0.0733 (LF)**
8	111	**0.2400 (HF)**	**0.1600 (HF)**	**0.0800 (LF)**
9	112	**0.2400 (HF)**	**0.1700 (HF)**	**0.0800 (LF)**
10	115	**0.2800 (HF)**	**0.1700 (HF)**	**0.0930 (LF)**
11	117	**0.2300 (HF)**	**0.1600 (HF)**	**0.0770 (LF)**
12	118	**0.2500 (HF)**	**0.1600 (HF)**	**0.0833 (LF)**
13	119	**0.2700 (HF)**	**0.1700 (HF)**	**0.0900 (LF)**
14	121	**0.2500 (HF)**	**0.1600 (HF)**	**0.0840 (LF)**
15	122	**0.2300 (HF)**	**0.1600 (HF)**	**0.0770 (LF)**
16	123	**0.2300 (HF)**	**0.1500 (LF)**	**0.0770 (LF)**
17	124	**0.2500 (HF)**	**0.1700 (HF)**	**0.0840 (LF)**
18	200	**0.2300 (HF)**	**0.1500 (LF)**	**0.0770 (LF)**
19	203	**0.2300 (HF)**	**0.1500 (LF)**	**0.0770 (LF)**
20	212	**0.2100 (HF)**	**0.1400 (LF)**	**0.0700 (LF)**
21	221	**0.2100 (HF)**	**0.1400 (LF)**	**0.0700 (LF)**
22	230	**0.2100 (HF)**	**0.1400 (LF)**	**0.0700 (LF)**
23	231	**0.2200 (HF)**	**0.1500 (LF)**	**0.0740 (LF)**

* HF high frequency, LF low frequency, and VLF very low frequency.

The new measure high frequency error is calculated as

$HFerror\ (r_H = \frac{HF}{total})$

Therefore, the high frequency error r_H for MVF algorithms shown in Table 3 are

1. Rosenstein $r_{H_r} = \frac{23}{23} \times 100\% = 100\%$
2. Wolf $r_{H_W} = \frac{11}{23} \times 100\% = 47.83\%$
3. Mazhar-Eslam $r_{H_M} = \frac{1}{23} \times 100\% = 4.34\%$

The figure 9 shows the bar diagram of the high frequency error.

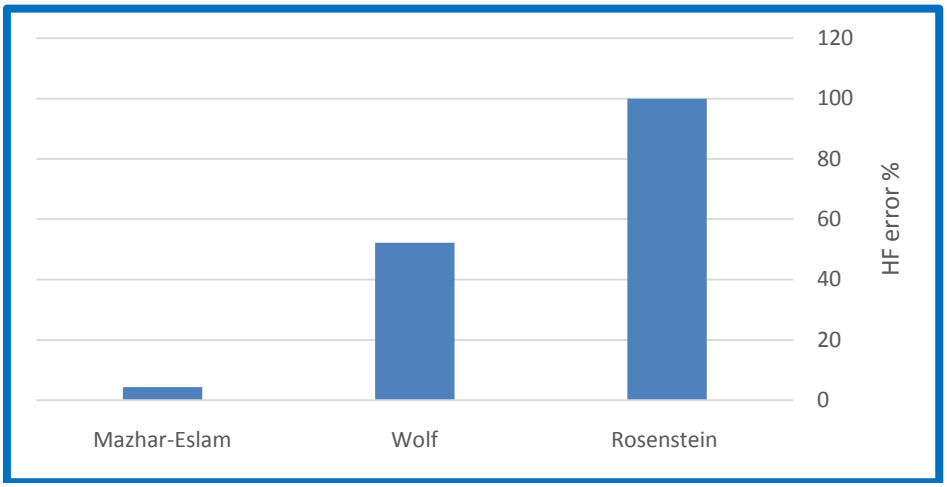

Figure 9. High frequency error of MVF.

By reference to MIT-BIH arrhythmia database medical records, it is found that the cases in Table 3 are critical cases as shown in figure 11. Some cases have Ventricular ectopy like 102, 104, 106, 107, 109, 119, 123, 221, and 231 as seen in figure 12, and some of these cases have Supraventricular ectopy like 111, 112. In addition, some of these cases in Table 3 have both Supraventricular ectopy and Ventricular ectopy like 118, 124, 200, and 203. The Ventricular ectopy and Supraventricular ectopy lie in the HRV low frequency band, because of their MVF is low. Table 3 shows that the Mazhar-Eslam algorithm for MVF $\overline{\Omega_M}$ is more precise than Wolf and Rosenstein algorithms. Also, the Mazhar-Eslam algorithm shows that the selected cases from MIT-BIH are in the low frequency range as its spectrum variation indicate ($\Omega_M < 0.16$ Hz). The Wolf algorithm has less precision than Mazhar-Eslam algorithm. Wolf observed incorrect band for cases 111, 112, 115, 117, 118, 119, 121, 122, 124, and 231 because they are not in the high frequency band as it shows but they are in the low frequency band as mentioned before. The worst and imprecise algorithm is Rosenstein as it shows all cases in the high frequency band. Thus, the Mazhar-Eslam is a recommended algorithm for HRV analysis.

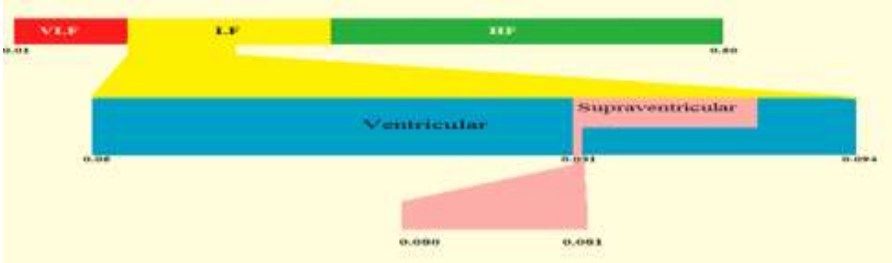

Figure 10. The MVF diagnosis diagram for ventricular and supraventricular

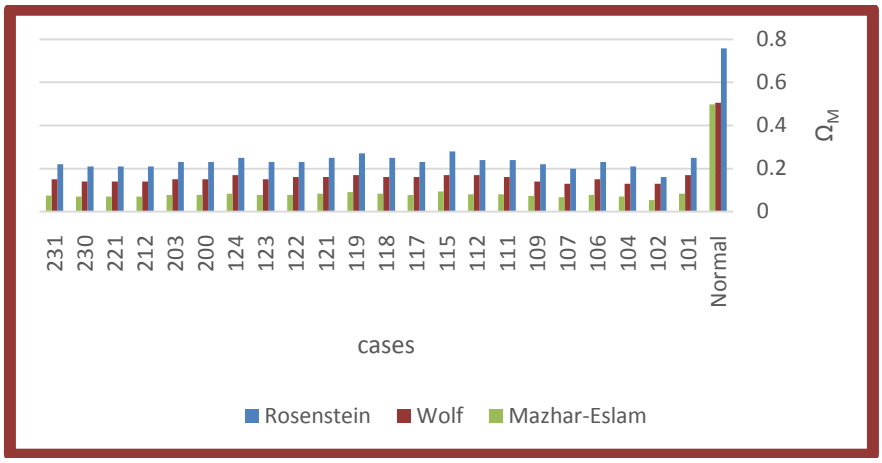

Figure 11. The MVF of the given cases.

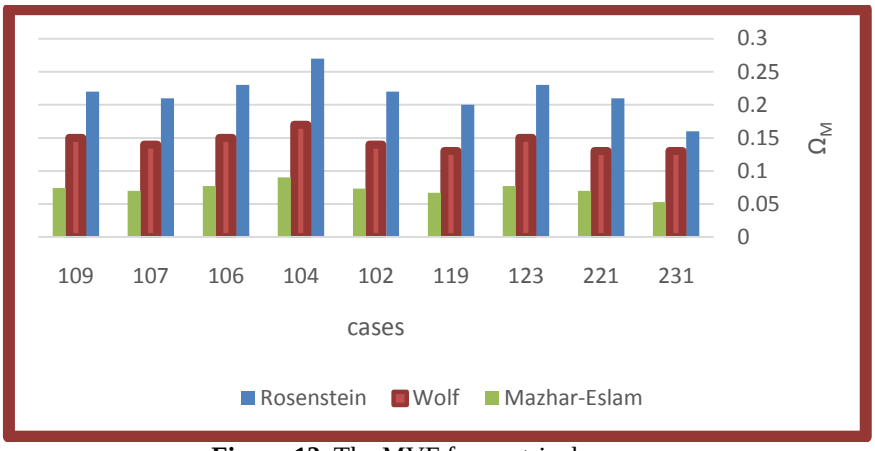

Figure 12. The MVF for ventricular cases

VIII. CONCLUSION

Heart Rate Variability (HRV) is reported in several cardiological and non-cardiological diseases. Also, it has a prognostic value and is therefore very important in modelling the cardiac risk. The HRV is a stochaotic signal that remains highly controversial. In order to have utmost importance, HRV needs a sensitive measure to analyse it. It is concluded that Mazhar-Eslam variability mean frequency (MVF), is a versatile and more precise qualitative SED measure of HRV sensitivity than others. The Rosenstein algorithm provided less sensitive MVFestimates than the Wolf algorithm to capture differences in local dynamic stability from small gait data sets. The data supported the idea that this latter outcome results from the ability and inability of the Wolf algorithm and Rosenstein algorithm, respectively, to estimate adequately MVF of attractors with an important rate of convergence as those in gait.

Therefore, the Mazhar-Eslam algorithm appears to be more qualitative and appropriate to evaluate local dynamic stability from small gait data (SED) sets like HRV. Increase in the size of data set has been shown to make the results of the Mazhar-Eslam algorithm more suitable, although other means as increasing the sample size might have a similar effect. The Mazhar-Eslam algorithm uses the merits of the Discrete Wavelet Transform (DWT) instead of Fats Fourier Transform (FFT) unlike Rosenstein and Wolf. The Mazhar-Eslam algorithm cares for all SED variants especially the small ones like that are in HRV. These SED variants may contain many important data to diagnose diseases as R-R interval has many SED variants. Thus, the Mazhar-Eslam algorithm for MVF ($\overline{\Omega_M}$) taking determination all of Ω_Ms is characterized by its high SED robust nest, and precise qualitative predictor. The Mazhar-Eslam algorithm presents a new chapter for HRV diseases diagnosis. It contains a positive part for HRV as it is stochaoticsignal.The next **Table 4** discusses the sensitivity and accuracy of MVF algorithms as it is clear the Mazher-Eslam is the best MVF algorithm for HRV.

Table 4. SED of MVF algorithms.

Cases No.	Mazher – Eslam (M-E)	Wolf (W)	Rosenstein (R)	SED
112, 101, 124, 119 and 115	0.0800, 0.0830, 0.0840, 0.0900, 0.0930	0.1700	0.2400, 0.2500, 2500, 2700, 2800	ME> W>R
102, 107 and 104	0.0530, 0.0667, 0.0700	0.1300	0.1600, 0.2000, 02100	ME> W>R
117, 122, 111, 118 and 121	0.0770, 0.0770, 0.0800, 0.0833, 0,0840,	0.1600	0.2300, 0.2300, 0.2400, 0.2500, 0.2500	ME> W>R
212, 221, 230 and 109	0.0700, 0.0700, 0.0700, 0.0733	0.1400	0.2100, 0.2100, 0.2100, 02200	ME> W>R
231, 203, 200,123 and106	0.0740, 0.0770, 0.0770, 0.0770, 0.0770	0.1500	0.2200, 0.2300, 0.2300, 0.2300, 0.2300	ME> W>R

The Poincaréplot is another sensitive and accurate technique that can be used for analyzing and predicting HRV. The Poincaréplot is a powerful and sensitive tool. It depends on statistical calculations. The plot and calculations represent the healthy case by a large ellipse area and very small for critical diseases cases. The Poincaréplot needs a suitable period to analyzing HRV. The recommended period lies between 5 and 20 minutes. Although, the Poincaréis sensitive and useful tool for HRV visual pattern, it has limitation. This limitation comes from limitation of standard descriptors *SD*1 and *SD*2. For avoiding this limitation, the complex correlation measure CCM is used. As the theoretical definition of *CCM* it is clear that the correlation information measured in*SD*1 and *SD*2 is already present in *CCM*. However, this does not mean that, *CCM* is a derived measure from existing descriptors *SD*1 and *SD*2. *CCM* can be considered as an additional measure incorporating information obtained in *SD*1 and *SD*2. *CCM* is based on the autocorrelation at different lags of the time series hence giving an in-depth measurement of the correlation structure of the plot. Therefore, the value of *CCM* decreases with increased autocorrelation of the plot. In arrhythmia, the pattern of the Poincaré plots becomes more complex.

REFERENCES

[1]. Mazhar B. Tayel and Eslam I AlSaba. Robust and Sensitive Method of Lyapunov Exponent for Heart Rate Variability. International Journal of Biomedical Engineering and Science (IJBES), Vol. 2, No. 3, July 2015. pp 31 -48

[2]. Mazhar B. Tayel, Eslam I AlSaba. Review: Linear Techniques for Analysis of Heart Rate Variability. International Journal of Engineering Science Invention, Volume 5 Issue 2, February 2016. pp 71 – 79.

[3]. Mazhar B. Tayel and Eslam I AlSaba. Review: Nonlinear Techniques for Analysis of Heart Rate Variability. International Journal of Research in Engineering and Science (IJRES), Volume 4 Issue 2, February. 2016. pp 45 – 60.

[4]. PAN, J. Tompkins, W. J. Areal-time QRS detection algorithm. IEEE transaction on biomedical engineering. Volume 32.pp 230 – 236.

[5]. Rangayyan, R. Biomedical Signal Analysis : a case-study approach. Piscataway, New jersey: IEEE Press New york, 2002. (IEEE Press series on biomedical engineering).

[6]. MEHTA, S. S.; SAXENA, S. C.; VERMA, H. K. Computer-aided interpretation of ECG for diagnostics. International Journal of Systems Science, volume 27. 1996. pp43 – 58.
[7]. SASIKALA, P, WAHIDABANU, R. Robust R Peak and QRS detection in Electrogardiogram using Wavelet Transform. International Journal of Advanced Computer Science and Applications. Volume 1. 2010. pp 48 – 53.
[8]. LOMB, N. R. Least-squares frequency analysis of unequally spaced data. Ap. Space Sci. volume 39. 1976.
[9]. SCARGLE, J. D. Studies in astronomical time series analysis. ii. statistical aspects of spectral analysis of unevenly spaced data. Astrophys. volume 263. 1982. pp 835 – 853.
[10]. Mazhar B. Tayel and Eslam I AlSaba. A NOVEL RELIABLE METHOD ASSESS HRV FOR HEART DISEASE DIAGNOSIS USING BIPOLAR MVF ALGORITHM. International Journal of Biomedical Engineering and Science (IJBES), Vol. 3, No. 1, January 2016. pp 45 – 56.
[11]. Mazhar B. Tayel and Eslam I AlSaba. A Declared Concept and a Proposed Algorithm to Assess HRV for Heart Disease Diagnosis. International Journal of Engineering Inventions, Volume 5, Issue 4, March 2016. pp 07 – 12.
[12]. Mazhar B. Tayel and Eslam I AlSaba. Statistical measurements for Comparison between Mazhar-Eslam Variability Frequency and other old Algorithms for accurate diagnosis of heart diseases. International Journal of Research in Engineering and Science (IJRES), Volume 4 Issue 3, March, 2016. pp 19 – 24.
[13]. Takens F. Detecting strange attractors in turbulence. Springer Lecture Notes in Mathematics vol 898, pp 366–81, 1981
[14]. Claudia Lerma, Oscar Infante, Hector Perez-Grovas and Marco V.Jose. Poincaré plot indexes of heart rate variability capture dynamic adaptations after haemodialysis in chronic renal failure patients. Clinical Physiology & Functional Imaging (2003) 23, pp72–80.
[15]. Mazhar B. Tayel, Eslam I AlSaba. Poincaré Plot for Heart Rate Variability. International Journal of Medical, Health, Biomedical, Bioengineering and Pharmaceutical Engineering Vol.9. No.9. September 2015. pp 657 – 660.
[16]. Karmakar C, Khandoker A, Gubbi J, Palaniswami M: Complex Correlation Measure: a novel descriptor for Poincaré plot. BioMedical Engineering OnLine 2009.
[17]. Rydberg A, Karlsson M, Hornsten R, Wiklund U. Can Analysis of Heart Rate Variability Predict Arrhythmia in Children with Fontan Circulation? PediatrCardiol 2008, 29:50-55.
[18]. Mazhar B. Tayel and Eslam I AlSaba. A Modified Method for Predictivity of Heart Rate Variability. Computer Science and Information Technology (CS&IT) - CSCP 2015. Vol.5, No.7, April 2015. pp 67 – 77
[19]. H.V. Sorensen and C.S. Burrus. Efficient computation of the DFT with only a subset of input or output points. IEEE Transactions on Signal Processing, 41(3): 11841200, March 1993.
[20]. V. Moga, C. Ioana, I. Bonchis, Florina Parv, T. Ciocarlie, C. Tudoran, Mariana Moga, RodicaAvram. The clinical value of nonlinear dynamics parameters in the assessment of the arrhythmic risk. Journal of Experimental Medical & Surgical Research, CercetãriExperimentale& Medico Chirurgicale Year XVIII · Nr.3/2011 · Pag. 107 – 112